Available online at www.sciencedirect.com
ScienceDirect
Ceramics International 34 (2008) 1779–1782
CERAMICS INTERNATIONAL
www.elsevier.com/locate/ceramint

Behavior of some potassium tungstates in the course of electrochemical lithium insertion

A. Martínez-de la Cruz *, L.G. Castillo Torres

División de Estudios de Posgrado, Facultad de Ingeniería Mecánica y Eléctrica, Universidad Autónoma de Nuevo León, Pedro de Alba s/n, Ciudad Universitaria, CP 66451, San Nicolás de los Garza, N.L., Mexico

Received 11 January 2007; received in revised form 1 February 2007; accepted 6 July 2007
Available online 10 August 2007

Abstract

Electrochemical lithium insertion has been studied in K_2WO_4, $K_2W_3O_{10}$ and $K_2W_4O_{13}$ through galvanostatic intermittent titration technique. We have monitored structural changes in the host matrix as lithium insertion proceeds through in situ X-ray diffraction experiments. In particular, K_2WO_4 showed to be unable to insert lithium in appreciable amounts. The maximum amount of lithium inserted in each oxide leads to specific capacities of 18 Ah/kg for K_2WO_4, 220 Ah/kg for $K_2W_3O_{10}$ and 265 Ah/kg for $K_2W_4O_{13}$. Nevertheless, due to irreversible structural transformations in the host matrix, such capacities were dramatically lost after the first cycle.

Keywords: D. Perovskites; D. Transition metal oxides; E. Batteries; E. Electrodes

1. Introduction

The chemistry of ternary oxides of tungsten is very rich and many compounds can be formed in relation with the size and valence of the ions nominally present in the oxides [1]. The different stoichiometries observed are justified for the presence of ions of elements such as alkalines, alkaline earths, transition metals, and rare earths to form, according with their valence, a great variety of tungstates $M(WO_4)_n$ where $1 \leq n \leq 6$. The high oxidation state observed in tungsten atoms and the open crystalline structure that exhibit a lot of them have led to their study as hosts in lithium insertion reactions in the present work.

In particular we will explore different tungstates belonging to the system K_2O–WO_3. The system K_2O–WO_3 has been widely investigated since early years [2]. It is well known that different stoichiometric ratio K_2O:WO_3 lead to different phases with complex structures. Only in the region rich in WO_3 content ($\geq$50%) five phases exist, i.e. 1:1, 1:2, 1:3, 1:4 and 1:6. Their structural arrangements are based in WO_4 or WO_6 units leading to structures with some empty holes where lithium ions can be introduced through an insertion reaction. Due to difficulties in the synthesis process the oxides studied here to undergo lithium insertion were K_2WO_4 (1:1) $K_2W_3O_{10}$ (1:3), and $K_2W_4O_{13}$ (1:4).

In K_2WO_4 the structure can be described as WO_4 tetrahedron surrounded by an almost regular hexagon of potassium ions forming a structure [3]. Crystal structures of $K_2W_3O_{10}$ and $K_2W_4O_{13}$ involved a more complex WO_6 octahedra arrangement. In $K_2W_3O_{10}$ four WO_6 octahedra are joined to form W_4O_{18} units by sharing edges, and five WO_6 octahedra to form a W_5O_{24} unit by sharing corners. These kinds of groups are linked by sharing corners building a framework of the $W_3O_{10}{}^{2-}$ anion [4]. It forms a very open structure with large tunnels occupied by potassium atoms and small triangular tunnels empty (see Fig. 1a). Taking into account the small ionic radii of lithium, it may be inserted in these tunnels through an insertion reaction. Finally $K_2W_4O_{13}$ is formed of distorted WO_6 octahedra, six of them are linked to form a six membered ring by sharing corners. Along *c*-axis the rings are linked by sharing its octahedra corner. A chain of WO_6 octahedra is connected to the hexagonal rings through octahedra linked by corners. The larger tunnels are occupied by potassium atoms and triangular tunnels (six by unit cell) are empty [5] (see Fig. 1b).

Recently in our group we have started a systematic study about the ability of similar bronzes to insert small ions like lithium [6,7]. In the present work we tested the possibility of

* Corresponding author. Tel.: +52 83 29 40 20; fax: +52 83 32 09 04.
E-mail address: azmartin@gama.fime.uanl.mx (A. Martínez-de la Cruz).

0272-8842/$34.00
doi:10.1016/j.ceramint.2007.07.001

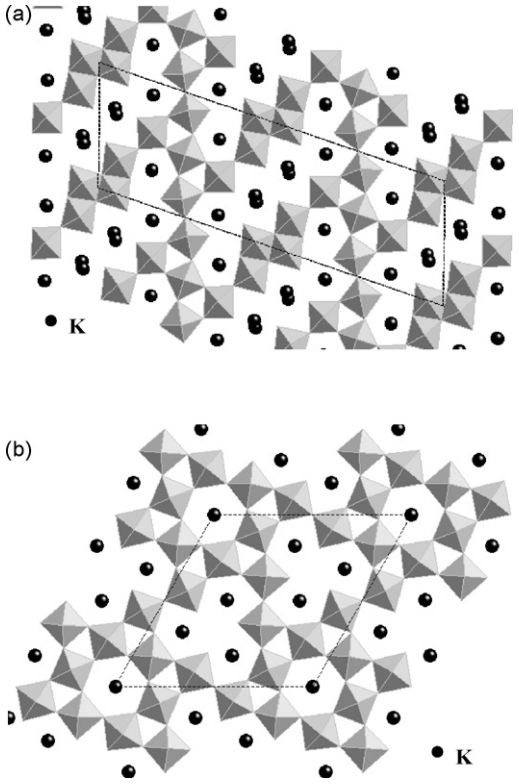

Fig. 1. Schematic representation of the (a) $K_2W_3O_{10}$ and (b) $K_2W_4O_{13}$ structures along the *b*-axis.

these phases to be used as insertion electrodes through electrochemical lithium insertion. In the same way, the influence of amount of tungsten in K_2O:WO_3 and crystalline structure in the characteristic parameters of the electrochemical cell, will be analyzed.

2. Experimental

The parent oxides were prepared by solid-state reaction between K_2CO_3 (Aldrich 99%) and WO_3 (Aldrich 99%). Mixtures in different stoichiometric ratios were prepared and slowly heated in an electric furnace from room temperature to 800 °C. In order to assure a complete reaction the mixture was kept at this temperature for 2 days. Structural characterisation of the pristine oxides, including lithiated compounds, were carried out by X-ray diffraction technique using a SIEMENS D-5000 diffractometer with Cu Kα (λ = 1.5418 Å).

Electrochemical experiments were performed in a galvanostat/potentiostat system MacPile II type. Different Swagelok type cells were assembled using lithium foil as negative electrode, and a 1 mol dm^{-3} solution of $LiClO_4$ in a mixture (1:1) of ethylene carbonate (EC) and diethoxyethane (DEE) as electrolyte. Pellets made of a mixture of tungstate/carbon black/binder in an 89/10/1 ratio were used as positive electrodes. Due to the high reactivity of metallic lithium, the assemblage of the cells was carried out in an argon filled glove box (MBraun) with a content in oxygen and water less than 1 ppm. The cells were cycled in galvanostatic conditions by using a current density of ±80 μA/cm^2.

The evolution of structural changes in the framework of the host as lithium insertion proceeded was followed in situ by X-ray diffraction. For this purpose we have used a laboratory made electrochemical cell that has a dual function: as sample holder and as electrochemical cell [8]. We run different cells in open circuit voltage conditions, applying a current density of 80–160 μA/cm^2 for 1.5–2.0 h and relaxing the cell for a similar time. Only when the system was in relaxation (variation of voltage with time smaller than 20 mV/h) X-ray diffraction data collection was carried out. This process was performed slowly due to poor crystallinity of lithiated phases. Typically we used a scan rate of 0.03°/5 s in the 2θ range from 20° to 60°.

3. Results and discussion

As product of the solid-state reaction between reactant oxides we obtained a blue powder for all compositions prepared K_2O:WO_3 (1:1, 1:3, and 1:4). In each case the corresponding X-ray diffraction pattern showed a good agreement with the previously reported for K_2WO_4, $K_2W_3O_{10}$, and $K_2W_4O_{13}$ [3–5]. On the basis of the results obtained by X-ray diffraction characterisation we have taken the three compositions prepared to perform electrochemical lithium insertion experiments.

3.1. K_2WO_4

Fig. 2 shows several charge–discharge cycles of a cell containing K_2WO_4 as active material, when it was discharged until 0.5 V versus Li^+/Li^0. The maximum amount of lithium incorporated in this oxide (~0.36 Li/K_2WO_4) led to a poor specific capacity of cell of 18 Ah/kg. As is shown in $E(x)$ plot, K_2WO_4 were unable to experiment a reversible lithium insertion. The origin of this irreversibility can be associated with the large plateau observed around 1.0 V versus Li^+/Li^0.

In order to characterise $Li_xK_2WO_4$ we have carried out in situ X-ray diffraction experiments during the discharge of the electrochemical cell. For all compositions studied the pristine crystalline structure of K_2WO_4 was maintained. This situation is not surprising taking into account the little amount of lithium

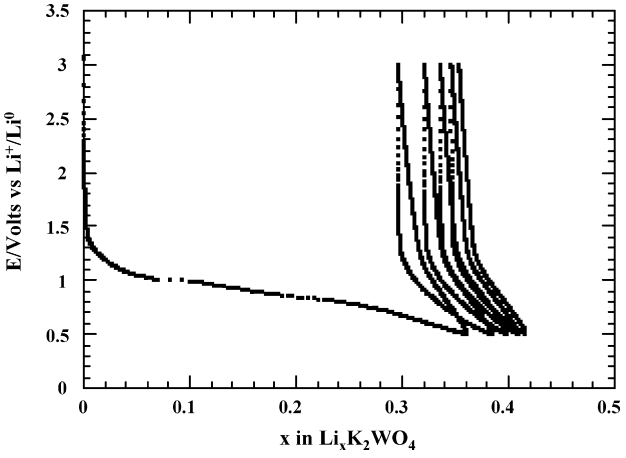

Fig. 2. Voltage–composition plot for several charge–discharge cycles of a cell with configuration Li//K_2WO_4 cycled under galvanostatic conditions applying a current density of ±80 μA/cm^2.

inserted. In this sense, the close crystalline structure of K_2WO_4 plays an important role in the difficulty to insert a major lithium amount.

3.2. $K_2W_3O_{10}$

Within phase diagram K_2O–WO_3, in the rich region of tungsten, different polytungstates with complex structures appear. The first polytungstate studied here corresponds with the composition $K_2W_3O_{10}$.

Fig. 3 shows the typical potential variation related with the amount of lithium inserted when some cells with configuration Li/electrolyte/$K_2W_3O_{10}$ were cycled between the potential range 3.0 and 0.5 V versus Li^+/Li^0. The maximum amount of lithium inserted under these conditions, approximately 6.4 lithium atoms per formula, leads to a specific capacity of 220 Ah/kg. Nevertheless, near of 80% of initial specific capacity was lost after the first charge–discharge cycle due to the inability of the system to remove 4.6 lithium atoms per formula during the charge process. The origin of this irreversibility can be found if we analyze the different processes involved in the insertion electrode during the charge–discharge of the cell. In this sense, the large plateau of semi-constant voltage observed along *E*–*x* plot of Fig. 3 can be associated directly with the irreversible nature of the reaction.

In order to follow structural evolution of $K_2W_3O_{10}$ as lithium insertion proceeds we have carried out in situ X-ray diffraction experiments during the discharge of the electrochemical cell. Fig. 4 shows the X-ray diffraction patterns of $Li_xK_2W_3O_{10}$ where $x = 1$–3. As reaction with lithium proceeds material become amorphous and for compositions with $x > 3$ all reflections of the pristine oxide are missing. On the basis of these results we can confirm that large plateau observed in Fig. 3 is due to an irreversible structural transformation of the host matrix.

3.3. $K_2W_4O_{13}$

Following in the direction of tungsten rich region in K_2O–WO_3 phase diagram appears the complex paratungstate

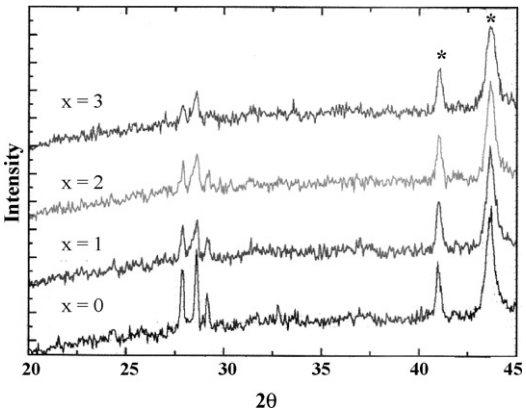

Fig. 4. X-ray diffraction patterns of $Li_xK_2W_3O_{10}$ obtained as electrochemical lithium insertion proceeded. *Peaks due to the sample holder.

$K_2W_4O_{13}$ (1:4). Although its structure shows that the larger tunnels are occupied by potassium atoms, each unit cell has six empty triangular tunnels where lithium can be inserted.

The voltage–composition plot obtained from the first charge–discharge cycle of a cell containing $K_2W_4O_{13}$ as active material is shown in Fig. 5. The lithium insertion proceeds through different processes as can be deduced from the evolution of the cell voltage with x in $Li_xK_2W_4O_{13}$. The maximum lithium inserted in $K_2W_4O_{13}$, i.e. ~10 lithium per formula, corresponds to a specific capacity for the cell of about 265 Ah/kg.

In order to know the origin of irreversible transition we have carried out the cycling of a cell Li/electrolyte/$K_2W_4O_{13}$ in the conditions above mentioned but until the minimum voltage limit of 1.2 V versus Li^+/Li^0. As can be observed in Fig. 6, the origin of system irreversibility is associated with the process previously labeled as A. In fact, the discharge of the cell at 1.2 V showed the reversible nature of the process to insert three lithium atoms in $K_2W_4O_{13}$.

According to its crystal structure described previously, lithium insertion of three lithium atoms per formula in $K_2W_4O_{13}$ is almost enough to fill the half of triangular tunnels present by unit cell. Octahedra rotation is favorable in this

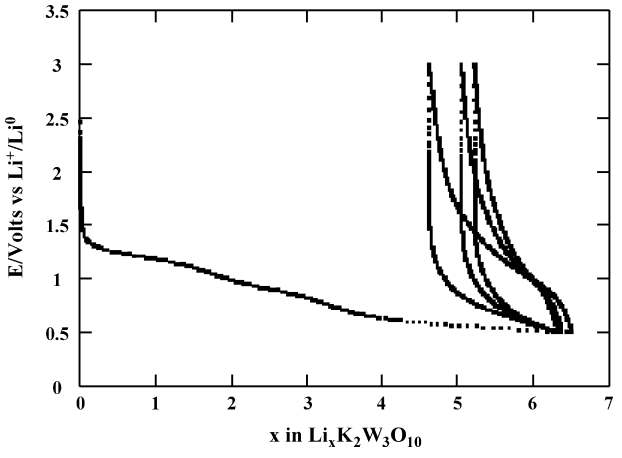

Fig. 3. Voltage–composition plot for several charge–discharge cycles of a cell with configuration Li//$K_2W_3O_{10}$ discharged under galvanostatic conditions applying a current density of ±80 μA/cm^2.

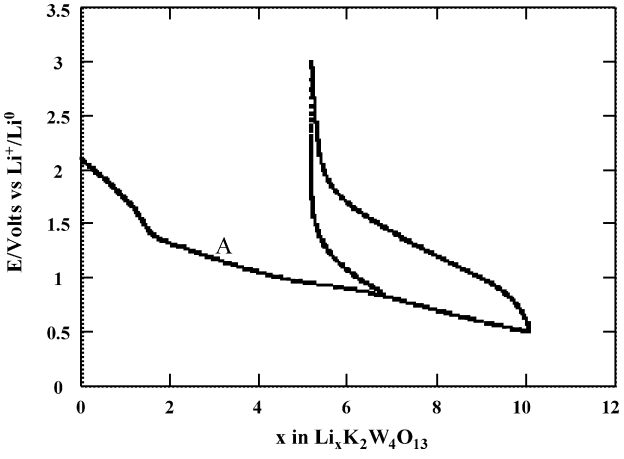

Fig. 5. Voltage–composition plot for a charge–discharge cycle of a cell with configuration Li//$K_2W_4O_{13}$ discharged under galvanostatic conditions applying a current density of ±80 μA/cm^2.

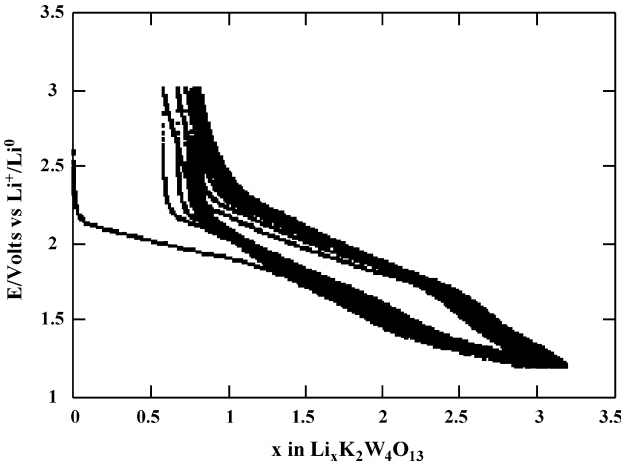

Fig. 6. Voltage–composition plot for several charge–discharge cycles of a cell with configuration Li//$K_2W_4O_{13}$ cycled under galvanostatic conditions. The cell was discharged until 1.2 V vs. Li^+/Li^0.

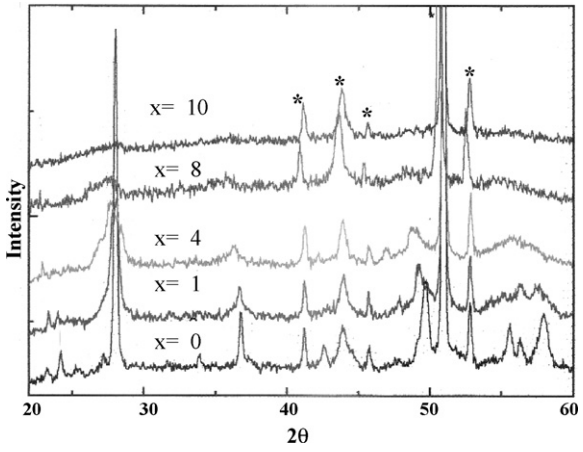

Fig. 7. X-ray diffraction patterns of $Li_xK_2W_4O_{13}$ obtained as electrochemical lithium insertion proceeded. *Peaks due to the sample holder.

structure taking into account that their octahedra are joined by corners, and insertion of three lithium atoms can be easily accepted through a structure relaxation. This situation can explain the reversible nature of the lithium insertion reaction in this range of composition ($0 \leq x \leq 3$).

Fig. 7 shows several X-ray diffraction patterns of composition $Li_xK_2W_4O_{13}$ ($0 \leq x \leq 10$). At low values of lithium insertion, i.e. $LiK_2W_4O_{13}$, the pristine matrix is maintained practically without increase on the values of cell parameters. As lithium insertion proceeds, see now $Li_4K_2W_4O_{13}$, some diffraction lines broads showing a beginning change in the original symmetry. For higher amount of lithium inserted, $Li_8K_2W_4O_{13}$ and $Li_{10}K_2W_4O_{13}$, X-ray diffraction showed that all diffraction lines of the pristine oxide disappear showing a total lost of the crystallinity. This situation was maintained when several compositions belonging to this range of composition were analyzed revealing thus the amorphous nature of the phase. In this sense, the composition reached of 8 and 10 lithium per formula in each case, suggests necessarily a lithium multi-occupancy model in the triangular tunnels with the corresponding degradation of the three-dimensional host network.

4. Conclusions

The maximum amount of lithium inserted in K_2O:WO_3 phases kept a correlationship with the WO_3 content. Phases with large amounts of tungsten ($K_2W_3O_{10}$ and $K_2W_4O_{13}$) exhibit very complex structures with large tunnels to insert lithium in them.

In particular, K_2WO_4 showed to be unable to insert lithium in appreciable amounts. The poor capacity developed for the electrochemical cell (18 Ah/kg) was associated with their closed structure. Although $K_2W_3O_{10}$ and $K_2W_4O_{13}$ developed high specific capacity of cell (220 and 265 Ah/kg, respectively), such capacity was dramatically lost after the first charge–discharge cycle due to irreversible structural changes.

The ability to insert lithium reversibly in the polytungstates was major when the minimum voltage value of the discharge was imposed at 1.2 V versus Li^+/Li^0.

Acknowledgements

We wish to thank to CONACYT for supporting the project 43800 and the Universidad Autónoma de Nuevo León (UANL) for its invaluable support through the project PAICYT 2006-2007.

References

[1] T. Ekström, R.J.D. Tilley, The crystal chemistry of the ternary tungsten oxides, Chem. Scripta 16 (1980) 1–23.
[2] L.L.Y. Chang, S. Sachdev, Alkali tungstates: stability relations in the systems A_2OWO_3–WO_3, J. Am. Ceram. Soc. 58 (1975) 267–270.
[3] A.S. Koster, F.X.N.M. Kools, G.D. Rieck, The crystal structure of potassium tungstate K_2WO_4, Acta Crystallogr. B 25 (1969) 1704–1708.
[4] K. Okada, H. Morikawa, F. Marumo, S. Iwai, The crystal structure of $K_2W_3O_{10}$, Acta Crystallogr. B 32 (1976) 1522–1525.
[5] K. Okada, F. Marumo, S. Iwai, The crystal structure of $K_2W_4O_{13}$, Acta Crystallogr. B 34 (1978) 3193–3195.
[6] A. Martínez-de la Cruz, F.E. Longoria Rodríguez, J. Ibarra Rodríguez, Electrochemical lithium insertion in the phosphate tungsten bronze $P_8W_{12}O_{52}$, Solid State Ionics 176 (2005) 2625–2630.
[7] F.E. Longoria Rodríguez, A. Martínez-de la Cruz, E. López Cuéllar, Behavior of the monophosphate tungsten bronzes $(PO_2)_4(WO_3)_{2m}$ ($m = 4$ and 6) in electrochemical lithium insertion, J. Power Sources 160 (2006) 1314–1319.
[8] R. Herrera Sánchez, L. Treviño, A.F. Fuentes, A. Martínez-de la Cruz, L.M. Torres-Martínez, Electrochemical lithium insertion in two polymorphous of a reduced molybdenum oxide (γ and γ′-Mo_4O_{11}), J. Solid State Electrochem. 4 (2000) 210–215.